

Using rodogram function to characterize hurst coefficient in rock profiles

<http://dx.doi.org/10.1590/0370-44672017710099>

David Alvarenga Drumond

<http://orcid.org/0000-0002-5383-8566>

Pesquisador

Universidade Federal do Rio Grande do Sul - UFRGS

Escola de Engenharia

Departamento de Engenharia de Minas

Belo Horizonte - Minas Gerais - Brasil

david.engminas.ufmg@gmail.com

Cláudio Lúcio Lopes Pinto

Professor

Universidade Federal de Minas Gerais - UFMG

Escola de Engenharia

Departamento de Engenharia de Minas

Belo Horizonte - Minas Gerais - Brasil

cpinto@ufmg.br

Abstract

Roughness is a fundamental feature to define rock deformability and resistance. A detailed characterization of discontinuity surface geometry is essential for understanding some of the rock's mechanical behaviors. Fractal geometry has been used by several authors to correlate parameters such as the Hurst coefficient for JRC (Joint Roughness coefficient) to better describe a surface geometry. Surface profiles might be characterized by a fractal dimension that represents the small scale of the geometric recurrence. In this paper, we propose to modify the methodology used to identify the Hurst coefficient incorporating the rodogram function in the JRC analysis. The proposed function is less influenced by drifting effects, and seems to be more precise than the commonly used variogram function. Robust mathematical models of spatial continuity can be a better alternative to characterize the roughness of rock discontinuities.

Keywords: rodogram, fractal dimension, variogram, joint roughness, Hurst coefficient.

1. Introduction

Joint roughness is one of the features responsible for strength, deformability, water flow and other rock mass properties. According to Lee (1990), discontinuities have an important influence on the deformational behavior of rock masses. Roughness directly influences the internal friction angle, dilatancy and peak shear strength. Such effects are highly dependent on the scale considered. There has been a considerable amount of research on rock roughness to understand its effects on rock deformability and strength. Raimbay *et al.* (2017) show that the variogram fractal dimension better describes the water and polymer solu-

tion flow in rock discontinuities. Li *et al.* (2017) present a fractal model for analyzing the shear behavior of large-scale opened rock joints.

The Joint Roughness Coefficient (JRC) is an important parameter for estimating rock quality (Barton, 1973). This parameter is commonly obtained by, visually, comparing the discontinuity profile against standard ones. The differences between actual and JRC proposed profiles has boosted the research on statistical geometry descriptions. Fractals is one of the most important methodologies for roughness description. Methodologies such as the box counting method

(Feder, 1988), variogram methodology (Orey, 1970), spectral analysis (Berry and Lewis, 1980), roughness length (Malinverno, 1990) and line scaling (Kulatilake, 1988) have been used to describe roughness profiles. Most of the relevant research studies on fractal dimension analyses have been done in the last decades of the twenty century.

Many authors have proposed several relationships associating fractal geometry, JRC and rock roughness (ODLING, 1994), (XIE, 1995), (BADGE, 2002). As discussed by Lee (1990), the relationship between JRC and the Hurst coefficient can be described as the empirical equation:

$$JRC = -0.87804 + 37.7844 \left(\frac{D-1}{0.015} \right) - 16.9304 \left(\frac{D-1}{0.015} \right)^2 \quad (1)$$

where D is the profile fractal dimension given by $D=2-H$. The equation is bounded for D values between (1.0046 and 1.013). The Hurst coefficient $0 < H < 1$ characterizes the self-similarity of rock profiles. A higher Hurst coefficient indicates lower rugosity while a lower Hurst coefficient indicates higher

rugosity. Experimental variograms are a common methodology used to estimate the Hurst coefficient.

The Hurst coefficient can be reasonably defined for stationary fields. A stationary behavior is commonly related to a stochastic process with mean and variance being constant along the

distance. However, drifting can be observed in most of engineering practical instances. It consists in one of the main problems in applying variogram methodologies to describe rugosity as much as in several other geostatistical features. Figure 1 illustrates a discontinuity profile obtained in a laboratory test.

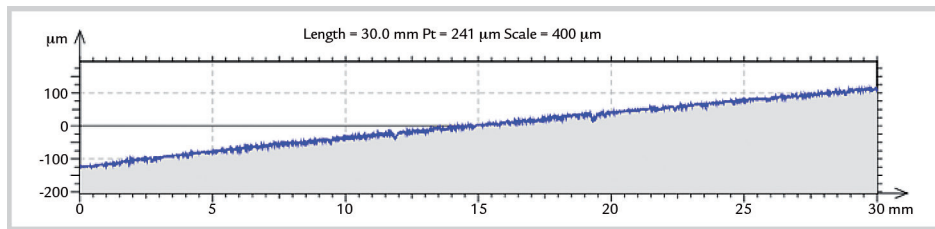


Figure 1
Discontinuity profile in a laboratory test.

This profile (Figure 1) is highly affected by the drift effect. Alternatively, the experimental data could be turned into a stationary field using a data transformation methodology. Figure 2 demonstrates the same profile after data transformation. For

this data transformation, linear regression was made to define the mean behavior of the profile, and simple rotation of the data provided the angle of a straight line, thus producing a new stationary behavior with constant mean. However, the mathemati-

cal methodology used to obtain a stationary field might reduce the rugosity scale and its variability (Vieira *et.al*, 2010). Even though stationarity can be reached mathematically, small trends should be considered since it is intrinsic to engineering problems.

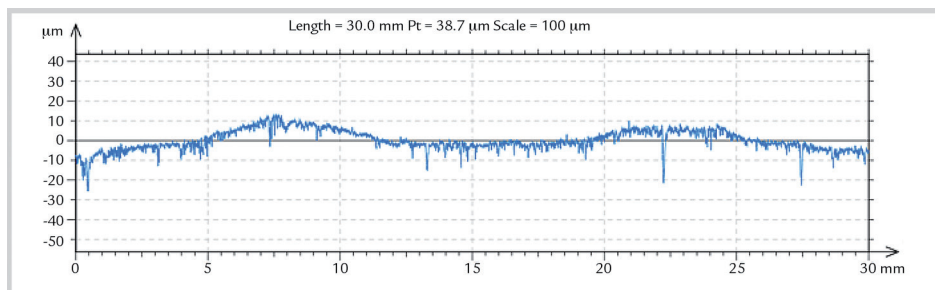


Figure 2
Discontinuity profile after data transformation. Note: scales used in Figure 1 and Figure 2 are not the same.

1.2 Fractal geometry

Maldebrodt (1977) introduced the concept of fractal geometry and the definition of “dimensions” that have been used in several areas of physics, mathematics and engineering. A line can be entirely represented in a 1-D space; an ideal plane in a 2-D and a solid, a cube for example, can be represented

by a 3-D space. Fractal dimension can be represented by a subdivision of a Euclidian dimension, and have mixed geometrical properties.

According to Kulatilake (1988), fractals can be understood as self-affined or self-similarity entities. A self-similar fractal is a geometric feature

that retains its statistical properties through various magnifications of itself. Differently, self-affined fractals change their statistical properties for different scales. It would not be reasonable to characterize rock roughness with self-similarity methodologies, due to its natural rock properties.

1.3 Generation of fractional Brownian profiles

Brownian motion profiles were created, using a constant Hurst coefficient, to compare the rodogram function estimation against the traditional variogram function.

Saupe (1988) describes several algo-

rithms for creating fractal geometries. The author discusses a well-known method to create fractional Brownian profiles called the Midpoint Displacement methodology. This proposition modifies the coordinates

of the line points based on a recursive function that redefines the midpoint of each sub segment. Figure 3 demonstrates the process of midpoint division. At level N=1, point 3 was created as follows:

$$x(3) = \frac{1}{2} [x(1) + x(2)] \quad (2)$$

$$y(3) = \frac{1}{2} [y(1) + y(2)] + D_1 \quad (3)$$

where D_1 is a normal random variable with mean =0 and variance = Δ^2_1 . The following points are defined by the recursive function:

$$x(4) = \frac{1}{2} [x(1) + x(3)] \quad (4)$$

$$y(4) = \frac{1}{2} [y(1) + y(3)] + D_2 \quad (5)$$

$$x(5) = \frac{1}{2} [x(3) + x(2)] \quad (6)$$

$$y(5) = \frac{1}{2} [y(3) + y(2)] + D_3 \quad (7)$$

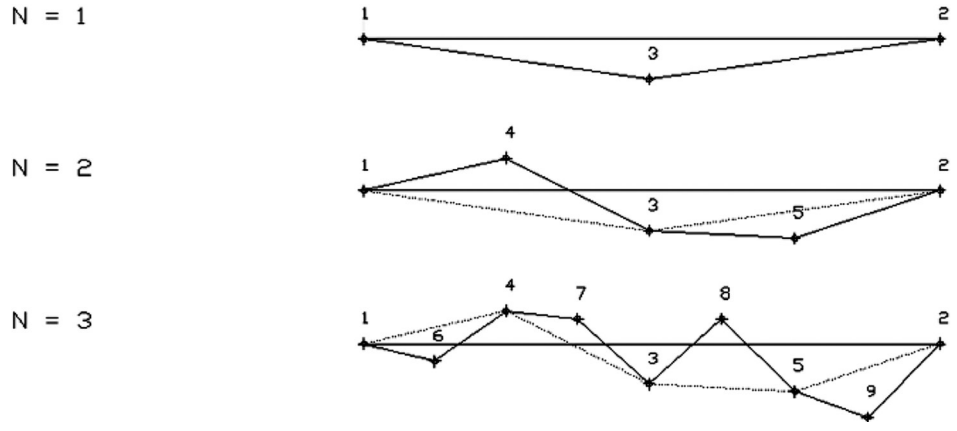


Figure 3 Brownian profile generation. At each level n , a midpoint is selected and redefined using a random function. At level $N=1$ segment is divided in two. At level $N=2$ segment is divided in 4. At level $N=n$, the segment is divided into $2n$ segments.

For each incremental level, the variance of D distribution modifies, according to:

$$\Delta_n^2 = \frac{\sigma^2 (1 - 2^{2H-2})}{(2^n)^{2H}} \quad (8)$$

where σ^2 is the initial variance, H is the Hurst coefficient and n is the

iteration number. Figures 4 and Figure 5 show examples of stationary and

non-stationary Brownian profiles, respectively.

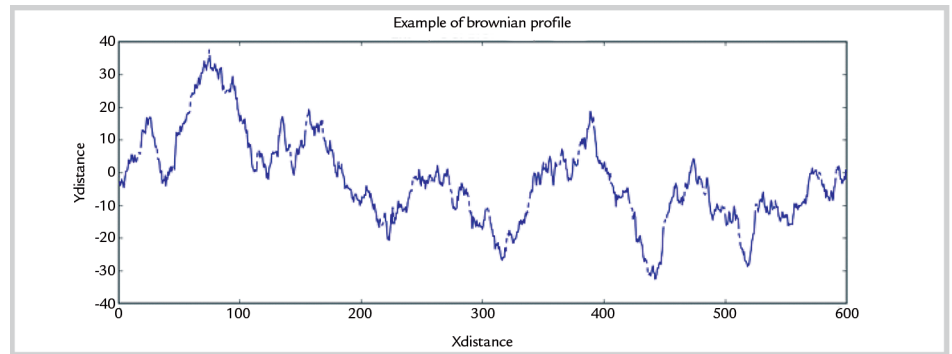


Figure 4 Example of Brownian profile. $\sigma^2 = 100$, $H = 0.6$, $n=10$. No Drifting.

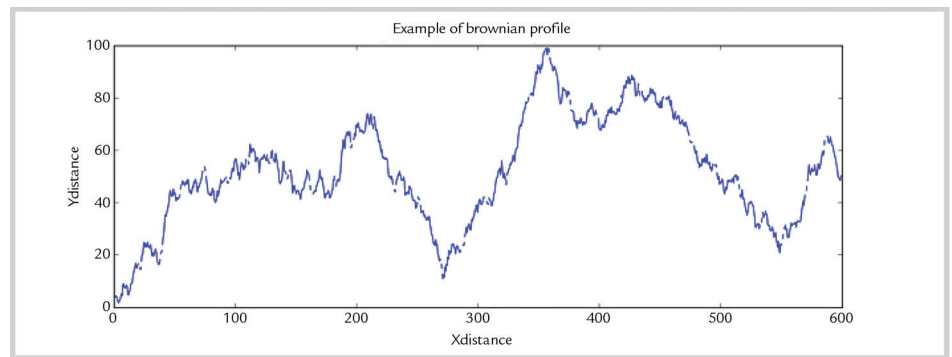


Figure 5 Example of Brownian profile with drift component. $\sigma^2 = 100$, $H = 0.6$, $n=10$. With Drifting.

1.4 Characterizing the Hurst coefficient using variogram and rodogram

Variogram can be defined as the expected value of the squared difference of regionalized random variables

$E[(Z_i - Z_{i+h})^2]/2$. According (KULATI-LAKE, UM e PAN, 1998) one can estimate the Hurst coefficient using a

variogram function with the following relationship:

$$2\gamma(x, h)_{\rightarrow h=0} = K_v h^{2H} \quad (9)$$

where K_v is a coefficient of proportionality, H is the Hurst coefficient and h , as in the classical geostatistic, is the distance vector between two samples. The Hurst component can be obtained by linearizing the log-log plot ($\log(2\gamma(x, h))$ and $\log(h)$).

The Rodogram function is a robust estimator that is less susceptible to non-stationary effects. According to Goovaerts (1997), this robust estimator may provide a clearer description of spatial continuities revealing their ranges and anisotropies

much better than the traditional variogram. This article proposes to estimate the Hurst coefficient using the Rodogram function defined as $E[(|Z_i - Z_{i+h}|)^{0.5}]/2$, where Z is the regionalized random variable, modifying Equation 9 into:

$$2\gamma_r(x, h)_{\rightarrow h=0} = K_v' h^{0.5H} \quad (10)$$

Figure 6 shows the mean square error versus exponents in equation 10. It seems that the choice of coefficient of 0.5 is a better alternative to

determine the Hurst coefficient using Rodogram function.

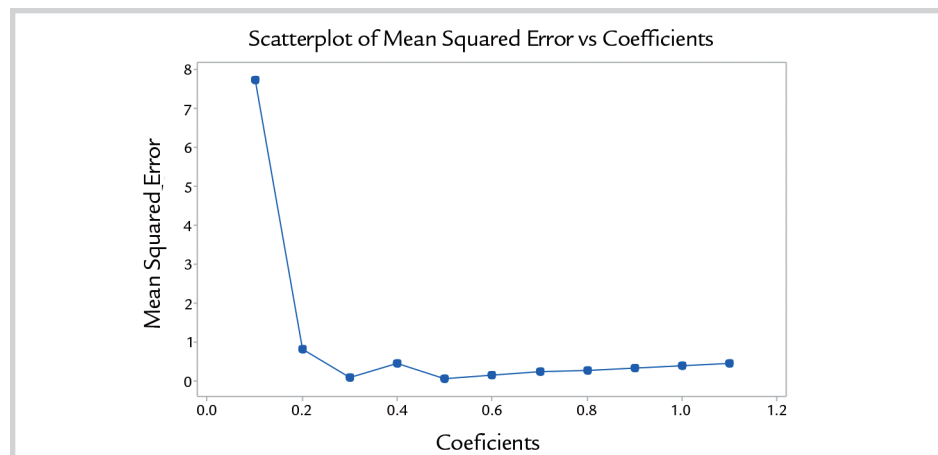


Figure 6 Scatterplot of mean squared error versus coefficients for a Hurst coefficient of 0.9 previously determined.

2. Methodology

To compare the variogram and rodogram methodologies, Brownian profiles have been generated. Table 1 presents the parameters used to generate a stationary Brownian profile using an initial horizontal base line. For the non-stationary profile generation, the y

coordinate of the end-point of the original baseline was modified according to a chosen drifting angle. A drifting angle in a Brownian profile can be simply defined as the arctangent of the difference in yfinal and ystart divided by the difference of xfinal and xstart. An initial Hurst coef-

ficient of 0.6 was used as a standard value. The objective here is to estimate the Hurst coefficient on this profile using traditional variogram and rodogram methodologies. Python programming was used to generate the Brownian profiles according to the same algorithm showed in section 1.3.

Brownian Profile Parameters

(x,y) start	(0.0)
(x,y) final (without drifting)	(600.0)
Hurst coefficient	0.6
Initial st deviation	10

Table 1 Brownian Profile parameters. Hurst coefficient was imputed as constant.

Variogram and rodogram log plots were used to define the best linear fitting points as shown in Figure 7. Hurst coefficients were estimated

using 5 lags of 10 unities of size. According to Kulatilake (1988), different lagsizes cause differences in the Hurst estimator; therefore, a standard

parameter for spatial continuity functions was used for better comparison between the rodogram and variogram methodologies.

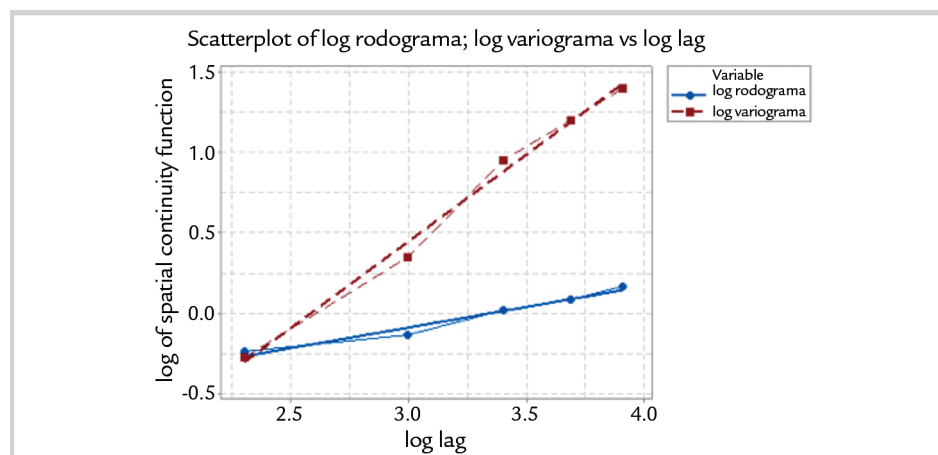


Figure 7 Spatial continuity functions log plot –(Seven points).

Groups of 10 Brownian profiles-generated with the same imposed Hurst coefficient, the same variability and the same drifting angle ($H_{input} = 0.6$ and $\sigma = 10$) were used to compute the statistics of the estimated Hurst coefficient. The estimation

error was calculated for both spatial continuity functions (rodogram and variogram).

The Hurst coefficient average error for different drift values were calculated as the difference between the expected value, defined by the mean of estimated values,

and the true value, previously used for creating the roughness profiles.

Rodogram and variogram Hurst coefficient error were plotted to evaluate their response to the drifting profile. Drifting degrees varying from zero to 30 were

used in these plots.

Finally, the error was graphically

analyzed for different Hurst coefficients for a non-drifting surface, to compare

the differences between the variogram and rodogram methodologies.

3. Results and discussion

The averages of the Hurst coefficient calculated for different drifts are presented in Table 2. The drifting

angles were obtained by increasing the n-point vertical distance using a factor of 2. The original profile gen-

erated was obtained using a constant Hurst coefficient of 0.6.

Hurst component ($H_{input} = 0,6$ and $\sigma = 10$) x estimation error

drift	Average H Rodogram	Average H Variogram	Relative H ¹ Rodogram error	Relative H ² Variogram error
0	0.59	0.57	3.33%	6.67%
0,48	0.58	0.57	5.00%	8.33%
0,95	0.57	0.56	8.33%	10.00%
1,91	0.57	0.56	6.67%	11.67%
3,81	0.59	0.57	3.33%	8.33%
7,59	0.59	0.58	1.67%	6.67%
14,93	0.62	0.60	-5.00%	1.67%
28,07	0.67	0.66	-20.00%	-16.67%

Table 2

Hurst coefficient error ($H_{input} = 0.6$ and $\sigma = 10$) for different drift values.

¹Relative error = |True value - Estimated value|/True Value

²Relative error = |True value - Estimated value|/True Value

The average error of the Hurst coefficients for each drift are presented in Figures 8,9, and 10. The rodogram estimator presents smaller errors than

the variogram estimator for drift angles under approximately 10°. Higher drifts, where the variogram can be considered a better estimator are not usually found

in rugosity profiles. It should also be pointed out that for drift angles over around 10°, the error increases rapidly for both methodologies.

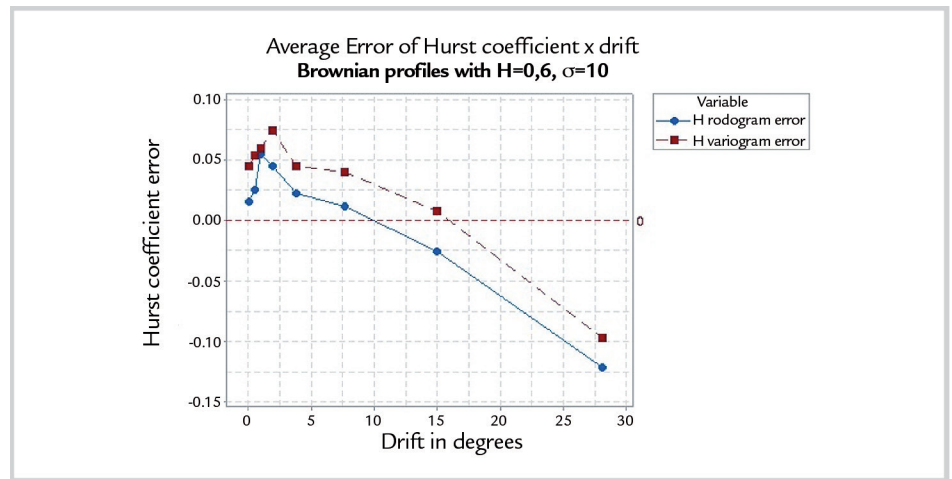


Figure 8

Average Error of Hurst coefficient vs drift. Hurst coefficient 0.6 and $\sigma = 10$.

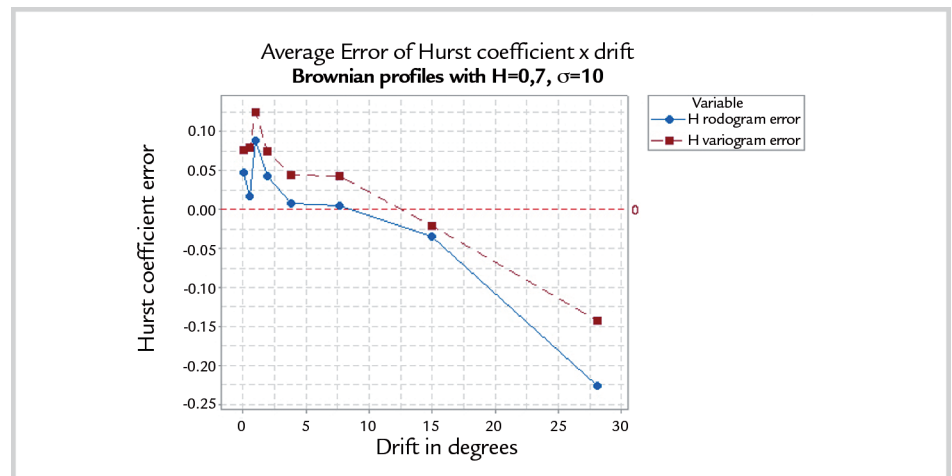


Figure 9

Average Error of Hurst coefficient by drift. Hurst coefficient 0.7 and $\sigma = 10$.

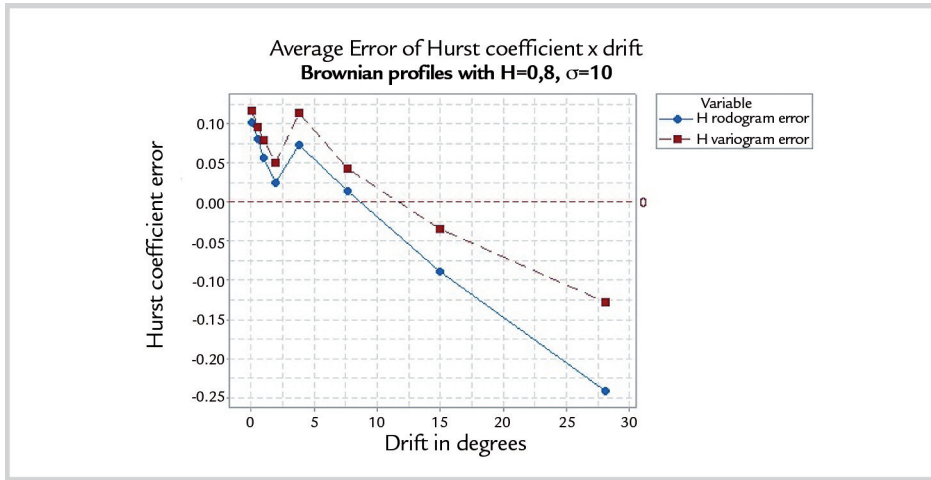


Figure 10
Average Error of Hurst coefficient by drift. Hurst coefficient 0.8 and $\sigma=10$.

When a stationary problem has been considered, the variogram is a more precise estimator than the rodogram

(average rodogram error is less than variogram average error), but less accurate (the rodogram coefficient of

variation is greater than the variogram), as shown in Table 3 .

standartdesviation	Hurst	rodogram	variogram	rodogram	variogram
		cv	cv	error	error
10	0.6	0.084	0.064	0.014	0.033
10	0.5	0.082	0.074	0.066	0.015
10	0.4	0.117	0.103	0.018	0.014
10	0.2	0.142	0.131	0.034	0.032
7,5	0.6	0.090	0.078	0.029	0.036
7,5	0.5	0.113	0.099	0.055	0.016
7,5	0.4	0.124	0.135	0.021	0.011
5	0.2	0.163	0.149	0.042	0.037
5	0.4	0.169	0.143	0.014	0.014
5	0.6	0.095	0.100	0.024	0.026
5	0.8	0.074	0.071	0.056	0.080
average	0.473	0.114	0.104	0.024	0.027

Table 3
Rodogram and variogram errors and coefficient of variation for different standard deviations, and inputHurst coefficients. No drift has been considered.

Figure 11 presents the Hurst coefficient error for the different profiles generated. It seems that the average error of linear estimators (variogram and rodogram) are only deslocated by a constant defined by the exponent of the spatial

continuity function as demonstrated in Figure 10. As discussed by Kulatilake (1988), the error presented by the variogram methodology increases as the Hurst coefficient increases. Rodogram methodology seems to be better defined for high

Hurst coefficient values and lower drifts, less than 10 degrees. Considering that rock roughness profiles can be defined at these terms, the Rodogram methodology can be a better alternative for describing rock mass discontinuity roughness.

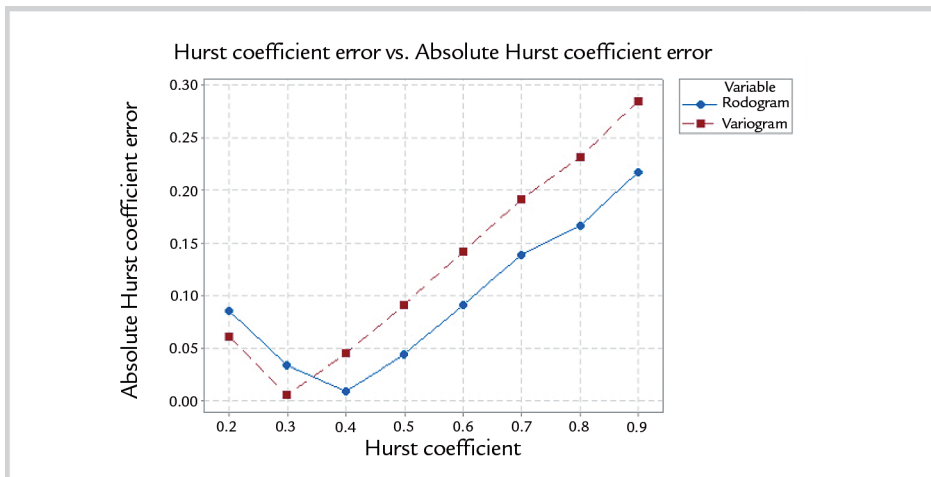


Figure 11
Hurst coefficient error vs Hurst coefficient. Average values for different Brownian profiles with standard variations equal 5, 7.5 and 10. 500 simulations used for each Hurst coefficient. No drift was inserted.

4. Conclusion

In this study, the spatial continuity function rodogram was proposed to estimate the Hurst coefficient of rock discontinuity roughness profiles instead of the variogram commonly used. Brownian profiles were created imposing a Hurst coefficient which has been forward estimated using models of spatial continu-

ity. Rodogram methodologies presented errors lower for small drifts and small fractal dimensions when compared to variogram methodologies. Variograms were less accurate than rodograms when small drifts are considered (lower than 10°). For higher drift values, neither the variogram or the rodogram methodol-

ogy presented good results for Hurst parameter determination. When no drift was considered, both the rodogram and variogram essentially presented the same error for a Hurst coefficient lower than 0.6. Variogram and rodogram methodologies failed to describe the Hurst coefficient for profiles presenting higher roughness.

References

- BADGE, M. N. E. A. Rock mass characterization by fractal dimension. *Engineering Geology*, v. 63, p. 141-155, 2002.
- BARTON, N. Review of a new shear strength criterion for rock joints. *Engineering Geology*, v. 7, p. 287-332, 1973.
- BERRY, M. V., LEWIS, Z. V. On the Weirstrass-Mandelbrot fractal function. Proceedings of the Royal Society of London A. *Mathematical, Physical and Engineering Sciences*, v. 370, 1980.
- FEDER, J. *Fractals*. New York: Plenum Press, 1988.
- GOOVAERTS, P. *Geostatistics for natural resources evaluation*. [S.l.]: Oxford University Press on Demand, 1997.
- KULATILAKE, P. H. S. W., UM, J., PAN, G. Requirements for accurate quantification of self-affine roughness using the variogram method. *International journal of solids and structures*, p. 4167-4189, 1998.
- LEE, Y.-H. E. A. The fractal dimension as a measure of the roughness of rock discontinuity profiles. *International Journal of Rock Mechanics and Mining Sciences & Geomechanics Abstracts*, v. 27, 1990.
- LI, Y. et al. A Fractal model for the shear behaviour of large-scale opened rock joints. *Rock Mechanics and Rock Engineering*, 50, p.67-79, 2017.
- MALINVERNO, A. A simple method to estimate the fractal dimension of a self affine series. *Geophysical Research Letters*, v. 17, p. 1953-1956, 1990.
- MANDELBROT, B. B. *Fractals*. [S.l.]: John Wiley & Sons, Inc, 1977.
- MATSUSHITA, M., O. S. On the self-affinity of various curves. *Journal of the Physical Society of Japan*, p. 1489-1492, 1989.
- ODLING, N. E. Natural fracture profiles, fractal dimension and joint roughness coefficients. *Rock mechanics and rock engineering*, v. 27, p. 135-153, 1994.
- OREY, S. Gaussian sample functions and hausdorff dimension of level crossings x. *Wahrsheninkets theorie verw. Gebierte*, p. 249-256, 1970.
- RAIMBAY, A. et al. Fractal analysis of single-phase water and polymer solution flow at high rates in open and horizontally displaced rough surfaces. *International Journal of Rock Mechanics & Mining Sciences*, 92, p.54-71, 2017.
- SAUPE, D. *Algorithms for random fractals*. New York: Springer, 1988.
- VIEIRA, et al. Detrending non stationary data for geostatistical applications. *Bragantia, Campinas*, v. 69, 2010.
- XIE, H. Fractal estimation of joint roughness coefficients. *Chinese Science Abstracts*, p. 55, 1995. (Series B).

Received: 30 June 2017 - Accepted: 5 April 2018.